IEEE Transactions on Aerospace and Electronic Systems, Volume 60, Issue 2, April 2024, pp. 1597-1611
DOI: 10.1109/TAES.2023.3337190

Dynamic Knowledge-based Tracking and Autonomous Anomaly Detection

Jianduo Chai, Shaoming He*, Hyo-Sang Shin and Antonios Tsourdos

***Abstract*—This paper presents a study on the problem of region surveillance in complex terrain using an unmanned aerial vehicle (UAV), and proposes a novel framework for on-road ground target tracking and detection of anomalous driving behavior with the assistance of domain-constrained information. In order to improve the accuracy of ground target tracking, terrain information is extracted and incorporated as constraints into the tracking process. To account for the dynamic changes in terrain-constrained information, a sliding window approach leveraging a dynamic programming algorithm is employed for domain-constrained knowledge inference. To improve the autonomy and intelligence of the monitoring UAV, a mechanism for recognizing suspicious driving patterns is seamlessly integrated into the target tracking process with the aid of domain knowledge. The effectiveness of proposed method is validated using extensive numerical simulations.**

***Index Terms*—airborne surveillance, ground target tracking, dynamic terrain information, domain knowledge aided, dynamic programming, anomalous driving behavior detection.**

I. Introduction

With the rapid development of microelectronics and sensor technology, small-scale unmanned aerial vehicles (UAVs) have become more adaptive and flexible, leading to an increasing trend of using UAVs for both civilian and military purposes. These applications include, but are not limited to, region surveillance [1], [2], search and rescue [3], cargo delivery [4], and wildlife conservation [5]. For any of these applications, accurate localization regardless of the presence of sensor noise is the foundation for achieving satisfactory performance. In addition, the autonomous extraction of crucial information, such as anomalous behavior detection, using UAVs will improve the working efficiency significantly and free up manual labor [6]. Despite the significance of aforementioned aspects, the existing literature lacks satisfactory methods to address them, both comprehensively and effectively.

For accurate tracking without incurring dramatic computational demanding, an increasing number of researchers have adopted domain-knowledge aided method for airborne tracking applications [7]–[13]. Namely, this method requires prior knowledge about constraint information, which can be obtained from both intrinsic or extrinsic factors. By incorporating domain knowledge into target tracking process, the uncertainty space regarding state estimation is reduced, hence improving tracking accuracy. Technically, previous studies of this field can be broadly classified into three categories. The first category modifies the target or sensor model to incorporate constraint information intrinsically. This involves establishing target on-road dynamic model [12], [14] or incorporating constraints into sensor model as perfect measurements [15], [16], also known as pseudo-measurement method. To be specific, an one-dimension representation of road network was presented in [12] and terrain information was incorporated into tracking process through designing an on-road kinematic model. Reference [9], on the other hand, approximated the irregular road by multiple curvature segments and considered the external constraints as pseudo-measurements. However, this method may result in covariance matrix, thus increasing the possibility of numerical problems [17]. The second category involves forming on-road probability distributions through using 'directional process noise'. The works in [18] considered the constraints of topography information by leveraging the directional process noise. Similarly, the authors in [19] presented a variable structure multiple model particle filter (VSIMM-PF) and employed the road-constrained process to involve domain knowledge. However, this method only imposes soft constraints on state estimation, implying that constraint violation may occur occasionally. The third method incorporates domain constraints by devising constrained filters, such as constrained sequential Monte Carlo (CSMC) filter [20], [21], projection method [17], [22], moving horizon estimator (MHE) [23], norm constraint filter [24], optimization with T-FOT (trajectory function of time) [25], [26] and gain constraint filter [27].

However, these existing methods all encounter a pervasive hurdle in the accurate alignment of constraints with the intended target, particularly in the presence of dynamic constraint conditions [9], [25], [28]. This challenge, if not surmounted, can lead to significant degradation in system performance due to mismatching or ambiguity issue [29]. Although the interact multiple model (IMM) or variable structure IMM (VS-IMM) is commonly employed to identify the relevant domain information [18], [30], its implementation may entail extensive parameter tuning and can result in constraint switch delay, especially when the target traverses multiple constraints rapidly.

Once target state information is obtained via tracking, anomalies detection method is seamlessly applied so that UAV can detect suspicious behaviors autonomously. To this end, a wide spectrum of studies have been conducted over the past few years [6], [31]–[34]. Those studies primarily involve two solutions: single discrete state and sequence states analysis,

Jianduo Chai and Shaoming He are with the School of Aerospace Engineering, Beijing 100081, China.

Hyo-Sang Shin and Antonios Tsourdos are with the School of Aerospace, Transport and Manufacturing, Cranfield University, Cranfield MK430AL, UK.

*Corresponding author. Email: shaoming.he@bit.edu.cn.

Published by IEEE. This is the Author Accepted Manuscript issued with: Creative Commons Attribution License (CC:BY 4.0).
The final published version (version of record) is available online at DOI:10.1109/TAES.2023.3337190. Please refer to any applicable publisher terms of use.

also known as trajectory analysis method. By establishing ad hoc statistical model between current target state and anomaly definition, the single state analysis method calculates the corresponding anomalous level and extracts anomalous behaviors, such as over-speed, anomalous intention and direction reversal, etc. In particular, the works in [34], [35] defined a sigmoid function to calculate the threat value based on target's current state. A Gaussian-process-regression-based method was introduced in [36], which also considered domain constraints for airborne target tracking. Different from the first approach, trajectory analysis approach infers target behavior through all states within a given time window. This method generally formulates an expert definition of target behavior patterns, which are then leveraged to examine a given state sequence. To be specific, if the current data sequence matches any illegal driving pattern predefined, anomalous behavior is detected. The studies in [33] defined several typical driving behaviors to classify target behavior given a part of trajectory, and a fuzzy-decision-making process was then used to match the feature of behavior. Similarly, [6] proposed a regular-expressions-based approach to match the characteristic of target driving behavior.

Compared with trajectory analysis method, the single state analysis method can be less reliable [34], [37], as the judgment only based on a single data can be easily misled by even minor disturbances such as sensor noise. However, despite the robustness, trajectory method is also problematic under certain circumstances. Anomalous behavior may have multiple manifestations that are difficult to enumerate, resulting in the false alarm of suspicious behavior [6]. Moreover, the definition of certain target driver pattern is dependent on local environment [33]. For instance, the same action triggering alert for investigation in normal traffic may be considered 'allowed' during congestion. Besides, the trajectories with a similar shape may indicate quite different meanings under different tracking contexts, say a curve trajectory indicating lane-changing action on straight roads may correspond to lane-keeping behavior on winding roads.

To close above mentioned gaps in applications of UAV surveillance, this paper proposes a novel overall framework integrated with both airborne target tracking and anomalous behavior detection mechanism. The framework is based on a road-section-oriented concept, in which all measures, including domain information extraction, on-road state estimation, and suspicious behavior recognition, are centered around a single road section or combination of road sections. The state constraint information is modeled as a Hidden Markov Model [38] (HMM) and is inferred using a dynamic programming method. The constrained state of the ground target is then calculated with a projection method [17], and a de-noising method is presented to mitigate noise in the process of domain constraint information confirmation. An anomalous behavior recognition mechanism is seamlessly integrated by analyzing the target driving characteristics, which are represented by a combination of road sections.

The contribution of this paper is twofold: Firstly, we present a logic delay approach using sliding window to autonomously infer the relevant domain constrained information and estimate the constrained states within the corresponding time length. Secondly, an efficient anomalous behavior recognition mechanism is introduced. This method obtains the anomalous value of ground target by analyzing the rarity of target driving pattern, which is represented by lane section sequence.

The remaining content of this paper is structured as follows. In Section II, the mathematical model and definitions for terrain information, ground target, sensor, and anomalous behavior are formulated. Section III presents the methodology for inferring constraint information, integrating constraints, and performing a de-noising process. Section IV explains the principle of extracting driving patterns, generating data, and designing the anomaly detection mechanism. In Section V, the effectiveness of the proposed method is demonstrated through extensive numerical simulations, which show improvements in both tracking accuracy and recognition of suspicious driving behavior.

II. System model formulation

This section utilizes a method for extracting domain-specific information from a high-quality digital map by representing the traffic lanes as an embedded graph. It defines the ground target model under terrain constraints and sensor model, and also describes model leveraged for the anomalous driving behavior detection.

A. Terrain model

In this study, we simplify the digital map by approximating it as a 2-D embedded graph, with edges and vertices representing specific lanes. The objective is to extract a universal geography information set $\mathcal{M}$, which can be used to constrain the motion of the target by leveraging the edges and vertices of the graph. $\mathcal{M}$ includes geography information of all lanes in this region and is defined as

$$\mathcal{M} = \{\mathcal{L}_l, \mathfrak{d}_l | l = 1, \cdots, n_{\mathcal{L}}\} \tag{1}$$

where l represents the lane index, $n_{\mathcal{L}}$ represents the total number of lanes in surveillance region, $\mathcal{L}_l$ is the information collection of lane l and $\mathfrak{d}_l$ contains the heading direction information of lane l. For each lane l, we have

$$\mathcal{L}_l = \left\{ s_l^{i,i+1} | i = 1, \cdots, n_s^l \right\} \tag{2}$$

where $s_l^{i,i+1}$ represents the intermediate section between two adjacent lane vertices $v_l^i = \left[x_i^l, y_i^l\right]^T$ and $v_l^{i+1} = \left[x_{i+1}^l, y_{i+1}^l\right]^T$, n_s^l represents the total number of sections of lane l. There is a substantial body of literature regarding segmentation approaches for representing lanes, as shown in previous studies [9], [10], [29]. Typically, the lane is either represented by a series of line segments or curves, while both methods inevitably introduce model errors. In this study, we employ a linear segmentation method for the approximation since it is both convenient and computationally efficient to implement, and importantly, the model error is adjustable. As a result, each linear lane section can be represented as follows,

$$s_l^{i,i+1} = \left\{ (1-a)\, v_l^i + a v_l^{i+1} | a \in [0, 1) \right\} \tag{3}$$

To effectively control the model error, we adopt the concept of maximum direction change error δ_{max} from reference [29] to determine the segmentation frequency based on the curvature of a given lane. Accordingly, the heading direction of the line segment can be calculated as follows:

$$\theta_l^{i,i+1} = \tan^{-1}\left(\frac{y_{i+1}^l - y_i^l}{x_{i+1}^l - x_i^l}\right) \in \mathfrak{d}_l \tag{4}$$

For clarity, the terrain modeling process is depicted in Fig. 1. Note that this study assumes the movement of the ground target to be restricted to a 2-D plane, which although simplistic, is suitable for modeling purposes, but may not accurately reflect the true surveillance scenario. However, this 2-D tracking approach can be easily extended to 3-D tracking by employing multiple 2-D planes to provide a comprehensive depiction of the lane shape in the 3-D space.

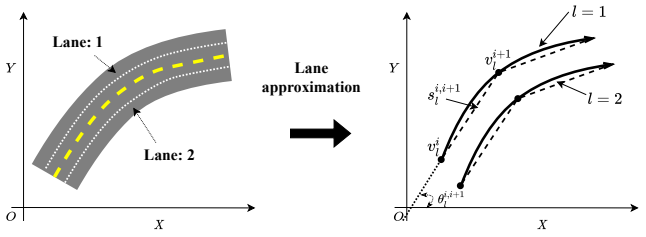


Fig. 1: Terrain model

B. Ground target and sensor model

The primary objective of target tracking is to accurately estimate the desired target state sequence $X_1^k = \{x_1, x_2, \ldots, x_k\}$ from sensor echoes $Z_1^k = \{z_1, z_2, \ldots, z_k\}$ that are expected to be corrupted by noise. Usually, the target state propagation is assumed to follow a Markov chain process, wherein the future state x_{k+1} is conditionally dependent only on the current state x_k, and is independent of previous states X_1^{k-1}. Similarly, we have

$$x_k = \mathbf{F}_k x_{k-1} + w_k \tag{5}$$

where w_k represents the process noise which is generally assumed to be white Gaussian with covariance $\mathbf{Q}_k$ (i.e., $w_k \sim \mathcal{N}(0, \mathbf{Q}_k)$). Given that on-road targets exhibit moderate maneuverability, we utilize a constant velocity model to enhance computational efficiency. Define $x_k = [x_k, \dot{x}_k, y_k, \dot{y}_k]^T$, and the state transition matrix $\mathbf{F}_k$ is represented as

$$\mathbf{F}_k = \mathbf{F} = \mathbf{I}_2 \otimes \begin{bmatrix} 1 & T \\ 0 & 1 \end{bmatrix} \tag{6}$$

where $\mathbf{I}_2$ represents a 2x2 identity matrix. In the target tracking process, domain-constrained knowledge is taken into consideration. Hence, the target state x_k and state propagation process noise w_k must adhere to the corresponding terrain constraints, hence we formulate the constraint models as follows,

$$\begin{aligned} C(x_k) &= 0, \\ \mathbf{Q}_k^c &= C(\mathbf{Q}_k) \end{aligned} \tag{7}$$

where $C(\cdot)$ represents a constraint relation exerted on the target state and the state transition process, and $\mathbf{Q}_k^c$ represents directional propagation noise. It is generally believed that the trace of the constraint matrix $\mathbf{Q}_k^c$ should be less than that of the covariance matrix $\mathbf{Q}_k$, as incorporating prior knowledge can help reduce the uncertainty space of state prediction and improve target tracking accuracy. However, when the ground target moves under complex terrain conditions, the performance can degrade significantly, particularly when dynamic constraint information switches quickly. This issue will be thoroughly addressed in Section III.

This study assumes that the small-scale UAV is capable of detecting the relative range r_k and azimuth β_k of the target with respect to its current position, similar to the monitoring model used in [9]. Therefore, given the current UAV position $x_k^U = \left(x_k^U, y_k^U\right)$ which is assumed prior-known, the intrinsic relation between the target state x_k and measurement z_k can be represented by the following nonlinear function as

$$\begin{aligned} z_k &= (r_k, \beta_k)^T = h(x_k) + \mathfrak{v}_k \\ &= \begin{pmatrix} \sqrt{\left(x_k - x_k^U\right)^2 + \left(y_k - y_k^U\right)^2} \\ \tan^{-1}\left(\frac{y_k - y_k^U}{x_k - x_k^U}\right) \end{pmatrix} + \mathfrak{v}_k \end{aligned} \tag{8}$$

where $\mathfrak{v}_k$ represents the sensor noise and is assumed to be white Gaussian with covariance $\mathbf{R}_k$ (i.e., $\mathfrak{v}_k \sim \mathcal{N}(0, \mathbf{R}_k)$).

Remark 1. *The UAV dynamics model is usually utilized in controller design for trajectory tracking, which has already been extensively addressed in contemporary research, as exemplified in [9], [39], [40]. In order to maintain the focus of our study, we assumed that the UAV is a point mass model without considering the UAV motion dynamics.*

C. Anomalies detection model

Different from previous studies that mainly rely on target trajectory analysis and specific behavior definition to recognize anomalous behavior, this paper proposes a method to extract target driving information by leveraging its interactions with local terrain, specifically, the lane sections. To achieve this, a fixed-length numerical sequence Se is used for target behavior representation and pattern matching with driving patterns collected in a database defined as $\mathcal{D}$. The rarity of a given driving pattern stored in Se is then calculated and defined as $A(Se|\mathcal{D})$. By linking the concept of behavior rarity with anomaly, the anomalous level of each driving behavior can be determined, as that the pattern which deviates so much from others as to arouse the suspicions that it was generated by a different mechanism [41]. The anomalous level of each driving behavior is defined as

$$\textbf{Respond} = \begin{cases} Alert, & \text{if } A(Se|\mathcal{D}) > u_1 \\ Monitor, & \text{if } u_2 < A(Se|\mathcal{D}) \le u_1 \\ Normal, & \text{if } A(Se|\mathcal{D}) \le u_2 \end{cases} \tag{9}$$

where u_1 and u_2 are constant parameters which describe the anomalous level of target behavior. The detailed methodology for defining driving patterns and recognizing anomalies is discussed in Section IV.

III. Domain Knowledge Aided Target Tracking

This section describes a method for inferring the correct domain knowledge using a dynamic programming approach within a sliding window. It also computes the on-road state of the ground target by applying and integrating constraints. To reduce data sequence noise, it introduces isolated points elimination and double window techniques.

A. Constraint information inference

In order to extract domain-constrained information that is imposed on the target state at each moment, a sliding window W with a fixed length Δt is used here. The terrain information sequence with respect to W is defined as

$$E_{t_e} = \{s_{t_e-\Delta t+1}, \cdots, s_k, \cdots, s_{t_e}\} \tag{10}$$

where t_e represents the ending time of window W and s_k is a random variable (RV) that links domain knowledge at k with the sample space $\mathcal{M}$ defined in Section II. For example, $s_k = s_l^{i,i+1}$ means that the ground target travels on the ith section of lane l at time k.

The terrain information set E_{t_e} is viewed as hidden states, which can only be inferred using observations. Thus this inference problem can be treated as a Hidden Markov Model (HMM), as illustrated in Fig. 2.

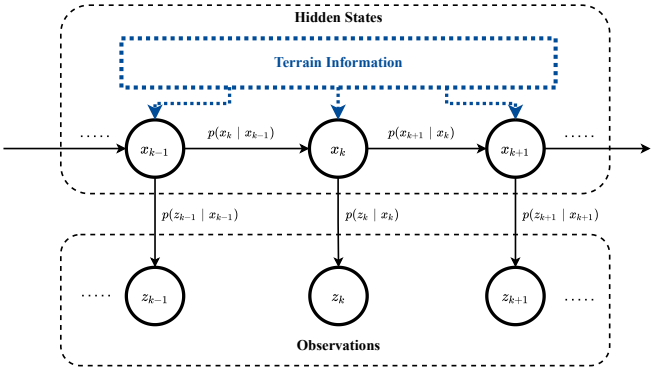


Fig. 2: HMM with terrain constraint

The observation sequence can be readily obtained via airborne sensor at t_e as

$$Z_{t_e} = \{z_{t_e-\Delta t+1}, \cdots, z_k, \cdots, z_{t_e}\} \tag{11}$$

To infer the relation between measurements and the traffic lanes, we need to calculate the geography position with respect to each measurement. To this end, the UAV position at each corresponding moment should be recorded, and the collection is defined as

$$U_{t_e} = \{x^U_{t_e-\Delta t+1}, \cdots, x^U_k, \cdots, x^U_{t_e}\} \tag{12}$$

and at any arbitrary moment k, the geography position, defined as p_k^z, is calculated as

$$p_k^z = [x_k^z, y_k^z]^T = \left[x_k^U + r_k \cos(\beta_k), y_k^U + r_k \sin(\beta_k)\right]^T \tag{13}$$

For each measurement, the vertical projection of p_k^z on arbitrary lane l is defined as $\hat{p}_k^z(l)$. The lane section on which the target is moving can also be obtained as $\hat{s}_k(l)$. Hence at each moment k, we have $n_{\mathcal{L}} + 1$ predictions about target current position, which are off lane: $(\hat{p}_k^z(0) = p_k^z, \hat{s}_k(0) : off - lane)$, on lane one: $(\hat{p}_k^z(1), \hat{s}_k(1))$, $\cdots$,and on lane $n_{\mathcal{L}}$: $(\hat{p}_k^z(n_{\mathcal{L}}), \hat{s}_k(n_{\mathcal{L}}))$. The prediction set Y_k at moment k can be represented as

$$Y_k = \{(\hat{p}_k^z(l), \hat{s}_k(l)) \,|l = 0, \cdots, n_{\mathcal{L}}\} \tag{14}$$

and the whole collection of target state and lane section predictions over the sliding window length Δt is obtained as

$$\{Y_k | k = t_e - \Delta t + 1, \cdots, t_e\} \tag{15}$$

The preference of target driving behavior such as lane keeping, lane changing, driving off road and driving onto road is defined as $\omega_{l'}^l$, which quantifies the transition probability from behavior l' to l. This value can be assigned by human expert based on specific tracking scenario. For instance, if off lane behavior is neglected, we can simply set $\omega_{l'}^l = 0$, for $\forall l = 0$. We can also assume that the ground target is inclined to perform lane keeping behavior instead of changing lanes frequently, thus we set ω_l^l to be much greater than $\omega_{l'}^l$ $(l \neq l')$.

It is evident that the number of possible terrain information flow with respect to the sliding window W grows exponentially with the time length Δt. To infer the correct domain knowledge combination without leading to huge computational complexity, a dynamic programming method named Viterbi algorithm [42] is applied to determine the most likely on-road state sequence of the ground target. This method obtains the likelihood of each data sequence by calculating the product of all states likelihood in the corresponding state sequence

Initial state $k = 1$, for $\forall l \in \{0, \cdots, n_{\mathcal{L}}\}$:

$$L_k^l = \log\left(p\left(z_k | \hat{p}_k^z(l)\right)\right) + \log\left(p\left(\hat{x}_k^l\right)\right) \tag{16}$$

Propagation $1 < k < t_e$, for $\forall l \in \{0, \cdots, n_{\mathcal{L}}\}$:

$$L_k^l = \max_{l' \in \{0, \cdots, n_{\mathcal{L}}\}} \left(\log\left(p\left(z_k | \hat{p}_k^z(l)\right)\right) + \log\left(\omega_{l'}^l\right) + L_{k-1}^{l'}\right) \tag{17}$$

Final state $k = t_e$:

$$l_k = \arg \max_{l \in \{0, \cdots, n_{\mathcal{L}}\}} L_k^l \tag{18}$$

$$s_k = \hat{s}_k(l_k) \tag{19}$$

where $p\left(z_k | \hat{p}_k^z(l)\right)$ represents the likelihood density and is assumed to be Gaussian, and $p\left(\hat{x}_k^l\right)$ with $k = 1$ represents the initial density of state at lane l. l_k in Eq. (18) is a RV which is the target traveling lane index at moment k. The domain information constraining target motion at each moment k is obtained as s_k in Eq. (19). By using the backward propagation, all the constraint information with respect to the state in the sliding window W, i.e., E_{t_e}, is subsequently extracted.

$$\mathbf{H}_k = \begin{bmatrix} \frac{x_{k|k-1}-x_k^U}{\sqrt{\left(x_{k|k-1}-x_k^U\right)^2+\left(y_{k|k-1}-y_k^U\right)^2}} & 0 & \frac{y_{k|k-1}-y_k^U}{\sqrt{\left(x_{k|k-1}-x_k^U\right)^2+\left(y_{k|k-1}-y_k^U\right)^2}} & 0 \\ \frac{y_k^U-y_{k|k-1}}{\left(x_{k|k-1}-x_k^U\right)^2+\left(y_{k|k-1}-y_k^U\right)^2} & 0 & \frac{x_{k|k-1}-x_k^U}{\left(x_{k|k-1}-x_k^U\right)^2+\left(y_{k|k-1}-y_k^U\right)^2} & 0 \end{bmatrix} \tag{23}$$

B. Constrained on-road filter

Once the terrain information is obtained, the next step is to formulate constraint functions and calculate all constrained target states within the sequence X_{t_e},

$$X_{t_e} = \{x_{t_e-\Delta t+1}, \cdots, x_k, \cdots, x_{t_e}\} \tag{20}$$

Given the fact that ground target may move through various terrain constraints, there are four typical behaviors that the target may perform during its journey, as listed as follows,

1) Section keeping behavior, $s_k = s_{k-1}$.
2) Section changing behavior (On the same lane), $s_k \neq s_{k-1}, l_k = l_{k-1}$.
3) Lane changing behavior, $l_k \neq l_{k-1}$.
4) Off lane behavior, $l_k = 0$.

These first three cases refer to the on-lane behaviors while the fourth case denotes the off-road behavior, which can be readily tracked with conventional unconstrained filter. In the first case, the ground target not only keeps the lane but also remains on the same lane section. In this case, both the target state and propagation process are constrained by the section information. In the second and third cases, the ground target breaks through the original constraints and demonstrates a certain level of maneuverability. In these cases, it is obvious that only the target state satisfies the terrain constraints while state propagation process noise should remain unconstrained or appropriately enlarged to account for the maneuverability.

To obtain the unconstrained state of target, the typical Bayesian principle is given as

$$p(x_k|Z_1^k) = \underbrace{\frac{p\left(z_k|x_k\right)}{p\left(z_k|Z_1^{k-1}\right)}}_{\text{state update}} \underbrace{\int dx_{k-1} p\left(x_k|x_{k-1}\right) p\left(x_{k-1}|Z_1^{k-1}\right)}_{\text{state prediction}} \tag{21}$$

with EKF steps as follows,

State prediction steps:

$$\begin{aligned} x_{k|k-1} &= \mathbf{F}x_{k-1} \\ \mathbf{P}_{k|k-1} &= \mathbf{F}\mathbf{P}_{k-1}\mathbf{F}^T + \mathbf{Q}_k \end{aligned} \tag{22}$$

and given UAV current position x_k^U, the Jacobian of measurement with respect to target state $x_{k|k-1} = \left[x_{k|k-1}, \dot{x}_{k|k-1}, y_{k|k-1}, \dot{y}_{k|k-1}\right]^T$ is obtained as $\mathbf{H}_k$ in Eq. (23).

State update steps:

$$\begin{aligned} \mathbf{S}_k &= \mathbf{H}_k\mathbf{P}_{k|k-1}\mathbf{H}_k^T + \mathbf{R}_k \\ x_k &= x_{k|k-1} + \mathbf{P}_{k|k-1}\mathbf{H}_k^T\mathbf{S}_k^{-1}\left(z_k - h\left(x_{k|k-1}\right)\right) \\ \mathbf{P}_k &= \mathbf{P}_{k|k-1} - \mathbf{P}_{k|k-1}\mathbf{H}_k^T\mathbf{S}_k^{-1}\mathbf{H}_k\mathbf{P}_{k|k-1} \end{aligned} \tag{24}$$

Next, we formulate constraint functions and apply them to the process of target state estimation. Following the inspiration of [28], we enforce that the position and heading direction of the ground target must satisfy the constraint information. Therefore, based on the map information extracted in Section III-A, suppose the correct domain knowledge related to target at moment k is $s_k = s_l^{i,i+1}$, then the terrain information such as section heading direction $\theta_l^{i,i+1}$ and vertex v_l^i can be readily obtained. We formulate the constraint functions for any arbitrary state x_k as follows:

$$\begin{aligned} &\underbrace{\begin{bmatrix} \tan\theta_l^{i,i+1} & 0 & -1 & 0 \\ 0 & \tan\theta_l^{i,i+1} & 0 & -1 \end{bmatrix}}_{\mathbf{D}} x_k \\ &= \underbrace{\left(\left[\tan\theta_l^{i,i+1}, -1\right]\left[v_l^i, 0_{2\times 1}\right]\right)^T}_{d} \end{aligned} \tag{25}$$

where the first term on the left-hand side of above equation represents constraint matrix, denoted as $\mathbf{D}$ and the second term is target state, and the term on the right-hand side represents a constraint bound, denoted as d. The problem of generating the constraint state can be reformulated as obtaining the maximum a posterior (MAP) of the state density that satisfies the given constraint relations,

$$x_k = \arg\max_{x_k} p\left(x_k|Z_1^k\right) \qquad \text{s.t. } \mathbf{D}x_k = d \tag{26}$$

This problem is readily solved with the Lagrange multiplier approach as suggested in [17], and the optimal result is derived as follows,

$$\begin{aligned} x_k &= \mathbf{J}_1 x_k + \mathbf{J}_2 \\ \mathbf{P}_k &= \mathbf{J}_1\mathbf{P}_k\mathbf{J}_1^T \end{aligned} \tag{27}$$

with the projection matrix $\mathbf{J}_1$ and location parameter matrix $\mathbf{J}_2$

$$\begin{aligned} \mathbf{J}_1 &= \mathbf{I}_4 - \mathbf{P}_k\mathbf{D}^T\left(\mathbf{D}\mathbf{P}_k\mathbf{D}^T\right)^{-1}\mathbf{D} \\ \mathbf{J}_2 &= \mathbf{P}_k\mathbf{D}^T\left(\mathbf{D}\mathbf{P}_k\mathbf{D}^T\right)^{-1}d \end{aligned} \tag{28}$$

where $\mathbf{I}_4$ is a 4×4 identity matrix. If the current position and velocity direction of the ground target satisfy the constraint equations, it is easy to prove that the one-step prediction $\mathbf{F}x_{k-1}$ also satisfies the constraint condition $\mathbf{D}\mathbf{F}x_{k-1} - d = 0$, corresponding to the state constrained model $C\left(x_k\right) = 0$ formulated in Section II. When the ground target remains on the same lane section during state propagation, the process noise should be constrained to comply with heading direction of the lane section. According to [43], the section directional noise can be calculated as follows,

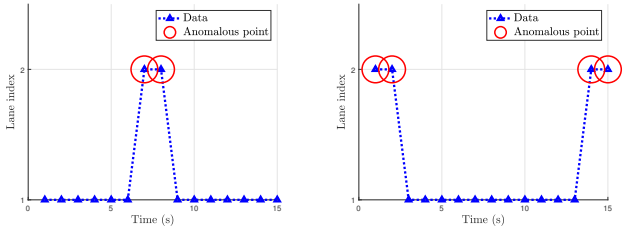
$$\mathbf{Q}_k^c = \left(\mathbf{I}_4 - \mathbf{Q}_k\mathbf{D}^T\left(\mathbf{D}\mathbf{Q}_k\mathbf{D}^T\right)^{-1}\mathbf{D}\right)\mathbf{Q}_k\left(\cdots\right)^T \tag{29}$$

where $\left(\cdots\right)^T$ represents the transposition of first term on the right-hand side of above equation. This directional noise

satisfies the constraint relation $\mathbf{D}\mathbf{Q}_k^c\mathbf{D}^T = 0$ and has the smallest covariance among all the possible constrained process noise, corresponding to the model $\mathbf{Q}_k^c = C(\mathbf{Q}_k)$ established in Section II.

C. Data noise mitigation

It is evident that the constrained state estimation process yields better target tracking performance than the unconstrained estimation process, as it considers more external information to overcome the space of uncertainty. However, this method heavily relies on the accuracy of the extracted constraint information, especially when complex terrain conditions are considered. A sliding window approach integrated with dynamic programming method is proposed for selecting the correct terrain information. Nonetheless, noise may occur and result in disastrous performance degradation. For illustration, two types of noise related to the lane confirmation result are shown in Fig. 3,



(a) Case one (b) Case two

Fig. 3: Data sequence noise

As shown in the first case, the pulse-like peak demonstrates a fluctuation occurring in an extremely short term, which is mainly caused by sensor noise. These anomalous fluctuations caused by noise generally have two features: 1. They only occur in a short term, and 2. they are surrounded by different points among which they share the same value. To detect the anomalous fluctuations and mitigate their negative impact on the tracking performance, we define T_{min} as the minimum length for a ground target to accomplish an overtaking behavior (switch to an adjacent lane and then switch back quickly), thus

$$\begin{cases} \text{Noise points confirmed,} & \text{if } N_A < \frac{T_{min}}{T} \\ \text{Overtaking behavior,} & \text{otherwise} \end{cases} \tag{30}$$

where N_A represents the number of subsequent isolated points sharing the same value, and it is believed that those points are caused by noise if the time length is not long enough to perform an overtaking behavior.

As shown in the second case, the method of eliminating isolated points mentioned earlier is not effective due to the insufficient information available in the current sliding window. This phenomenon is referred to as the edge effect, which is an inherent limitation of the proposed sliding window method. To mitigate this effect, there are two solutions. One is to devise an adaptive sliding window method that can automatically avoid having isolated points on the edges of each sliding window. Another solution involves designing a double window mechanism, which is adopted in this paper. The working principle of the double window method is shown in Fig. 4.

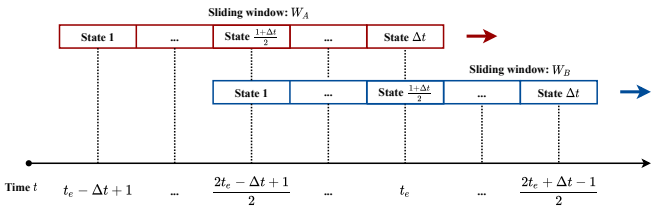


Fig. 4: Mechanism of double sliding window method

Each single window starts at the central moment of the other window, thus forming a complementary relation and mitigating the edge effect of each single window. To fuse the data from each sliding window, the posterior probabilistic density of window W_A and W_B at moment k are defined as $p\left(W_A|Z_1^k\right)$ and $p\left(W_B|Z_1^k\right)$, respectively. Based on Bayesian principle, we have:

$$p\left(W|Z_1^k\right) \propto p\left(z_k|W, Z_1^{k-1}\right) p\left(W|Z_1^{k-1}\right) \tag{31}$$

where $p\left(z_k|W, Z_1^{k-1}\right)$ denotes the likelihood density, while $p\left(W|Z_1^{k-1}\right)$ denotes the prior density. The likelihood density can be easily obtained thorough Eq. (21) as,

$$\begin{aligned} p\left(z_k|W, Z_1^{k-1}\right) &= p\left(z_k|x_{k|k-1}^W\right) \\ &\sim \mathcal{N}\left(z_k; x_{k|k-1}^W, \mathbf{R}_k\right) \end{aligned} \tag{32}$$

where $x_{k|k-1}^W$ is the predicted state with respect to window W. The confidence level on window W without information update using measurement is denoted as $p\left(W|Z_1^{k-1}\right)$. To mitigate the edge effect, a Gaussian distribution is devised for $p\left(W|Z_1^{k-1}\right)$, which can be expressed as

$$\begin{aligned} p\left(W_A|Z_1^{k-1}\right) &\sim \mathcal{N}\left(k; \frac{2t_e - \Delta t + 1}{2}, \left(\frac{\Delta t}{2\rho}\right)^2\right) \\ p\left(W_B|Z_1^{k-1}\right) &\sim \mathcal{N}\left(k; t_e, \left(\frac{\Delta t}{2\rho}\right)^2\right) \end{aligned} \tag{33}$$

where k represents the current moment and ρ is a parameter for deviation adjustment of the proposed distribution. The estimation result is obtained by fusing the estimation results of each sliding window using the following equation,

$$p\left(x_k|Z_1^k\right) = \sum_{W\in\{W_A,W_B\}} p\left(x_k|W, Z_1^k\right) p\left(W|Z_1^k\right) \tag{34}$$

with moment matching for state x_k^W and covariance $\mathbf{P}_k^W$ corresponding to each window W as

$$\begin{aligned} x_k &= \sum_{W\in\{W_A,W_B\}} p\left(W|Z_1^k\right) x_k^W \\ \mathbf{P}_k &= \sum_{W\in\{W_A,W_B\}} p\left(W|Z_1^k\right) \left(\mathbf{P}_k^W + \left(x_k^W - x_k\right)\left(x_k^W - x_k\right)^T\right) \end{aligned} \tag{35}$$

and the domain constrained knowledge E_{t_e} is then updated using the unit s_k^W with respect to each sliding window W as

$$\begin{aligned} W &= \arg \max_{W \in \{W_A, W_B\}} p\left(W | Z_1^k\right) \\ s_k &= s_k^W \end{aligned} \tag{36}$$

Due to the sliding window logic, a delay is unavoidable in tracking application. The delay length, however, is controllable and hence, researchers may use different window lengths to trade-off between tracking accuracy and efficiency, given specific application.

For clarity, the algorithm of proposed double window approach is given in Algorithm 1.

Algorithm 1 Overall structure of double window method

Require: Previous estimation results, current sensor echo z_k, domain knowledge $\mathcal{M}$ and current UAV position x_k^U

1: **while** Measurement z_k received **do**
2: **for** W_A **do**
3: Store measurement z_k in Z_{t_e}
4: Store current UAV position x_k^U in U_{t_e}
5: **if** Current moment $k = t_e$ **then**
6: Obtain on-road states and terrain information predictions via Eq. (15) with $\mathcal{M}$
7: Infer domain knowledge E_{t_e} via Eq. (16)-(19)
8: Obtain X_{t_e} and the corresponding covariance matrices using E_{t_e} via on-road state estimation in Section III-B
9: Isolated noisy points elimination in Section III-C
10: Update Z_{t_e} and U_{t_e}, set $t_e = t_e + \Delta t$
11: **end if**
12: **end for**
13: **for** W_B **do**
14: Repeat steps $3 \rightarrow 11$ with states corresponding to W_B
15: **end for**
16: **if** Any W is finished **then**
17: Obtain x_k and $\mathbf{P}_k$ for arbitrary moment k in W via data fusion in Section III-C
18: Update terrain inference E_{t_e} via Eq. (36)
19: **return** Target states and terrain reference results
20: **end if**
21: **end while**

Remark 2. *Though considering external information inference and constraints implementation with a delay logic, the proposed method's time complexity is comparatively lightweight. Let target state* $\mathrm{x}_k \in \mathbb{R}^{n_x}$*, the time complexity at each recursion is* $\mathcal{O}\left(n_x^3 + n_{\mathcal{L}}\right)$*. When considering the delay logic over length* Δt *for double window estimation, the corresponding time complexity is obtained as:* $2\Delta t\left(\mathcal{O}\left(n_x^3\right) + \mathcal{O}\left(n_{\mathcal{L}}^2\right)\right) + \mathcal{O}\left(\Delta t \cdot n_x^2\right) \in \mathcal{O}\left(\Delta t\left(n_x^3 + n_{\mathcal{L}}^2\right)\right)$*, which in fact, can be further reduced using efficient optimization method.*

Remark 3. *It is important to note that the proposed framework is extendable, and besides EKF, other state estimation methods such as constrained Monte-Carlo sampling method may also be feasible. Given specific application requirements, researchers may find suitable filter to trade-off between tracking accuracy and efficiency [44]. As for multiple target tracking application, the proposed method can be readily extended as well, via tackling the classic measurement-target allocation issue, generally known as data association problem, which has been well studied, especially in the field of radar application [45]–[48], and for simplicity, this issue will not be discussed in this research.*

IV. Anomalies detection

This section presents a method for defining target behavior using lane sections. It also proposes a pattern matching method and a database generation method for measuring the anomaly level of target behavior. Finally, it summarizes the overall framework of the anomaly detection mechanism.

A. Behavior definition

In this study, terrain information is obtained by approximating road lanes as continuous piece-wise sections. This information can be leveraged for detecting anomalous target behavior seamlessly. Each lane section is assigned with a unique number, and the driving behavior of a ground target during a specific time interval can be represented by a sequence of these numbers. For example, the lane sections can be encoded as shown in Fig. 5.

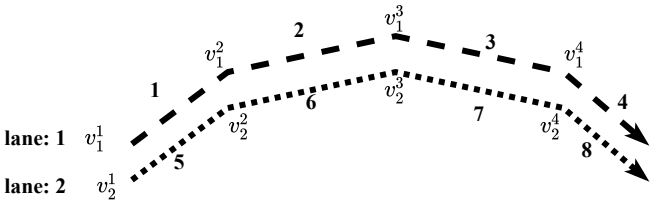


Fig. 5: Lane section encoding

Suppose that the sequence of lane sections on which the ground target moved is obtained as

$$\begin{aligned} Se(1) &= \text{‘1112233344’} \\ Se(2) &= \text{‘5566778’} \\ Se(3) &= \text{‘11223778’} \\ Se(4) &= \text{‘5562233778’} \end{aligned}$$

and with the aid of domain knowledge, the behavior of the ground target can be inferred from the lane section sequence. For instance, $Se(1)$ indicates that the ground target moves straightforwardly along lane 1, while $Se(2)$ suggests a similar action along lane 2. $Se(3)$ represents a lane-changing behavior as the target moves from lane 1 to lane 2, and $Se(4)$ is more likely an overtaking behavior in which the target switches to the adjacent lane and quickly switches back. Moreover, other information, such as traveling direction, speed magnitude, and the exact moment of lane change, can also be implied in the section sequences. This method can be effortlessly extended for analyzing multiple target behaviors, as the operator may infer reckless driving patterns or leader-follower relationships

by finding similarities among their corresponding road section sequences.

Note that there could be ambiguity when applying conventional trajectory analysis method [33] for behavior recognition. Specifically, there is a potential for the intended target to be mistakenly identified as executing lane change maneuvers by applying pure trajectory analysis method while actually, the target is following a path within a winding route, as shown in Fig. 6, which displays two driving scenarios. The first scenario (top) illustrates a lane-changing behavior, while the second scenario showcases a lane-keeping action. Despite the similarities in their driving trajectories, it is essential to note that the same trajectory can have different interpretations in distinct driving contexts. This underscores the potential challenges associated with trajectory analysis methods and highlights the significance of integrating external information.

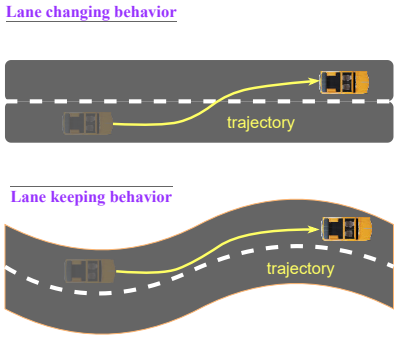


Fig. 6: Ambiguity in behavior recognition

B. Pattern matching

To effectively recognize suspicious behavior of ground target, a driving pattern rarity evaluation method is leveraged for comparing a given driving pattern with a target driving database. As substantial anomalous behavior occurs when the target exhibits a different maneuverability [6], we extract the feature of numeric strings by eliminating consecutively repeated numbers, shown as follows:

$$Se(4) = \text{‘5562233778’} \rightarrow Se^f(4) = \text{‘562378’} \tag{37}$$

where Se^f represents feature strings of the original string Se. The feature string Se^f is then transformed into a set of fixed-length numerical strings for ease of comparison, as follows:

$$Se^f(4) : \text{‘}\underbrace{5623}_{t_s=4}78\text{’} \rightarrow \begin{pmatrix} Se_1^s = \text{‘5623’} \\ Se_2^s = \text{‘6237’} \\ Se_3^s = \text{‘2378’} \end{pmatrix} \rightarrow \textbf{Examination} \tag{38}$$

where t_s represents the length of each split numerical string, and Se_n^s represents the nth split numerical string. The examination process is primarily aimed at assessing the degree of anomaly of a given split numerical string. Two methods can be utilized for this examination process: pattern matching and data-driven methods. For a fixed length of numerical string, making comparisons is simple and convenient. Thus, in this study, the pattern matching method is employed, which necessitates an extensive database encompassing a significant number of driving patterns related to the first digit of the split numerical string. For instance, for a string length of $t_s = 2$ related to road section 2, the most frequently occurring driving patterns are ‘23’: straight forward behavior, ‘26’: legal lane changing behavior, and ‘27’: legal lane changing behavior. Violation behavior is assumed to occur rarely and can then be easily detected. It is important to note that in most typical scenarios, a value of $t_s = 2$ proves to be adequate for the identification of aberrant actions pertaining to geographical position alterations, such as unauthorized lane changes, questionable off-road maneuvers, or instances of driving in the incorrect direction. Consequently, we employ $t_s = 2$ for validation purposes in the numerical simulations discussed in Section V.

The database can be generated autonomously by the UAV through surveillance data collection. However, in this paper, for simulation purposes while still maintaining authenticity, we define the transition between different road sections as a Markov chain model and generate target normal driving patterns through a random walk model, as illustrated in Fig. 7.

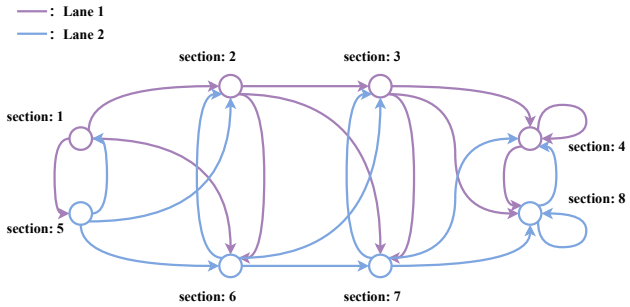


Fig. 7: Markov chain model of section switches

For each split string Se^s, its occurrence frequency can be obtained by searching for the same pattern within the string database $\mathcal{D}$, as $f(Se^s)$. Then the anomalous level of Se^s can be calculated as follows, based on its occurrence frequency and the total number of sequences N in the database:

$$A(Se^s|\mathcal{D}) \propto 1 - \frac{f(Se^s)}{N} \tag{39}$$

This equation represents the rarity of the given split numerical string compared to the frequency of occurrence of the same pattern in the driving pattern database. A backward process is then carried out to match the anomalous value of each Se^s with each time moment in the sliding window W, thus obtaining $A(Se|\mathcal{D})$. Next, according to the model Eq. (9) formulated in Section II, UAV will automatically take corresponding actions in response.

C. Overall framework of anomaly detection mechanism

For clarity, The mechanism for anomalous behavior detection is illustrated in Fig. 8. The input data are obtained through constrained on-road tracking, as described in Section III. The

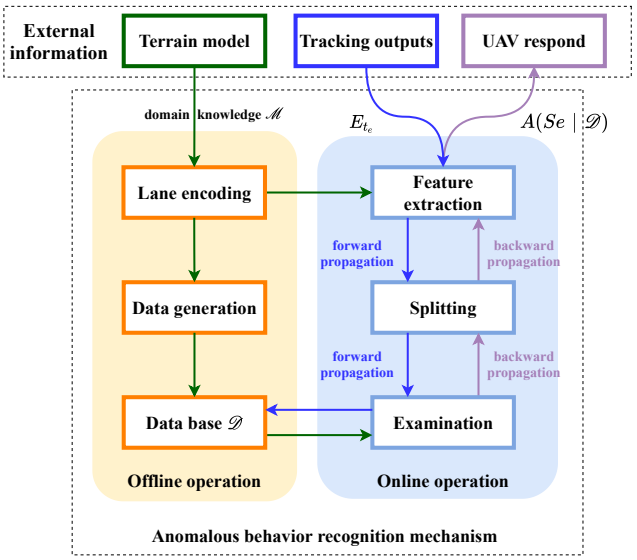


Fig. 8: Framework of anomaly detection mechanism

inputs consist of lane and section indexes collected within a sliding window as E_{t_e}. The output of the system is the anomalous level for each moment within the sliding window as $A\left(Se|\mathcal{D}\right)$. The overall mechanism is divided into two parts: an online operation (shown as the pale blue frame in Fig. 8) and an offline operation (shown as the pale yellow frame in Fig. 8). In the online operation, the features of the raw data are extracted and generated as Se^f. The feature numerical string is processed by the splitting part to generate a sequence of numerical strings Se^s with the same length. The examination part matches each split string with driving patterns collected in the database $\mathcal{D}$ and obtains the anomalous value through Eq. (39). The anomalous value of each split string is assigned to its first digit and matched with the raw data through backward propagation. In the offline operation, each lane section in the map is encoded with a specific digit to formulate an overall template, which is used for transforming the input data to the raw data used for online operation and is also used for generating data for the database $\mathcal{D}$. The database $\mathcal{D}$ not only receives driving patterns from initial data generation but also updates its database by collecting driving patterns from the online operation, hence customizing for local driving habits.

Remark 4. *Please note that the behavior recognition method is terrain-information-centered and is tailored for the domain knowledge based tracking application, as in one respect, the tracking application provides exact the information that recognition method needs for behavior inference, and in another, the behavior recognition mechanism demands highly robust estimation result, which is guaranteed by the incorporation of terrain constraint information in our tracking application.*

V. Numerical Simulation

This section evaluates the performance of proposed method through extensive simulations. The section first sets up the simulation scenarios and explains the evaluation metric and parameters. Then, we examine and compare the performance of the proposed methods, including both single and double sliding window methods, with unconstrained filter and constrained on-road filter with IMM logic. Finally, the effectiveness of proposed anomaly detection mechanism is demonstrated with numerical simulation.

A. Simulation setup

To evaluate the effectiveness of proposed domain-constrained filter and anomalous behavior recognition mechanism, a high-quality digital map is utilized to provide local terrain information, such as traffic lanes. The scenario includes four curved lanes with two different heading directions. The ground targets are permitted to either continue on their current road or switch to an adjacent lane with the same heading direction. However, any other lane-changing behaviors are considered illegal and regarded as anomalous behaviors.

Fig. 9 shows two ground target tracking scenarios for illustrative purposes. In the first scenario, the ground target enters the surveillance region at position A and travels to position B within 58s, at which point the tracking process ends. The target demonstrates mostly straight forward behavior during its journey, with only one overtaking behavior occurring at 20s and 30s, and therefore exhibits no anomalous behaviors. In contrast, the second scenario depicts a typical regulation violation circumstance, under which the target enters the region from position A and changes lane at 20s, before driving directly onto the contraflow lane at 40s. That lane changing action clearly violates the law and may result in severe consequences. A UAV is utilized for monitoring target behaviors in those two scenarios. Unless otherwise specified, the simulation parameters are summarized in Table I. The monitoring UAV maintains a consistent altitude of 50 meters with an average speed of 24 m/s. It is configured to track the intended target with an approximate distance that varies between 67 meters and 122 meters in bird's-eye view, as illustrated in Fig. 11.

TABLE I: Parameters required in the simulation

Parameter	Value
UAV sampling interval T (s)	0.5
Simulation length (s)	58
Process noise $\mathbf{Q}_k$	diag([20 20 20 20])
Sensor noise $\mathbf{R}_k$	diag([2 1/57.3])·diag([2 1/57.3])
Velocity range of ground target (m/s)	[14 20]
Slide window length Δt (s)	13
Initial state prediction	$[-213074.6991; 0; 6209735.658; 0]^T$
Initial covariance	diag([50 283 50 283])
Minimum time for overtaking T_{min}	3
Length of split numerical string t_s	2

To evaluate the tracking performance, we utilize two metrics, namely root mean squared error (RMSE) and mean distance error (MDE). RMSE is defined as the square root of the average of the squared differences between the estimated and ground truth positions of the target over a specified time interval. Mathematically, RMSE can be formulated as:

$$RMSE = \sqrt{\left(\frac{1}{N_s}\sum_{k=1}^{N_s}||p_k^e - p_k^t||_2^2\right)} \tag{40}$$



(a) Scenario one: normal driving behavior (b) Scenario two: abnormal driving behavior

Fig. 9: Surveillance scenarios

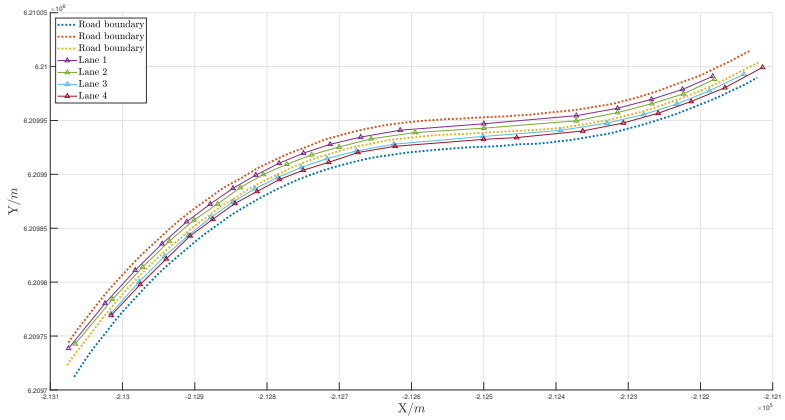


Fig. 10: Domain knowledge extraction

where N_s is the number of samples and $||\cdot||_2$ represents the Euclidean norm; p_k^e and p_k^t denote the estimated and ground truth positions at sample k, respectively. MDE is the average of the squared differences between the estimated and ground truth positions of the target over a specified time interval, which can be expressed as:

$$MDE = \frac{1}{N_s}\sum_{k=1}^{N_s}||p_k^e - p_k^t||_2 \tag{41}$$

B. Terrain information extraction

To extract domain constrained information from the given digital map, the lanes are approximated as multiple continuous piece-wise line sections, as suggested in [29]. The maximum heading direction error δ_{max} is set to be 3°. The approximation results are shown in Fig. 10, indicating that all curve lanes within the surveillance region are successfully divided into multiple line sections and are labeled from left to right in sequence as 1 to 4. Moreover, it is apparent that the frequency of segmentation is proportional to the lane curvature, which helps to mitigate the segmentation error.

C. Performance evaluation of single window tracker

According to the lane approximation process, it is evident that the ground targets travel through various constraints dynamically, which provides a challenge to existing road constrained filters as most of them only consider static constraint knowledge. To illustrate the effectiveness of the proposed method, both target tracking accuracy and terrain information inference results are evaluated. For emphasis, an unconstrained EKF and constrained on-road filter using IMM logic for constraint information inference are employed here. We select the first scenario for simulation, and the tracking result is depicted in Fig. 11. The result clearly reveals that the proposed method can persistently track the ground target regardless of the rapid change of domain constrained information. It is also observed that proposed method achieves better tracking performance than the unconstrained filter during most of the time. To further explore the tracking performance of the proposed method quantitatively, the MDE and mean terrain inference results of 1000 Monte Carlo simulations are shown in Fig. 12 and Fig. 13, respectively. Fig. 12 demonstrates that the proposed method outperforms EKF and constrained filter with IMM logic in terms of target tracking accuracy. Fig. 13

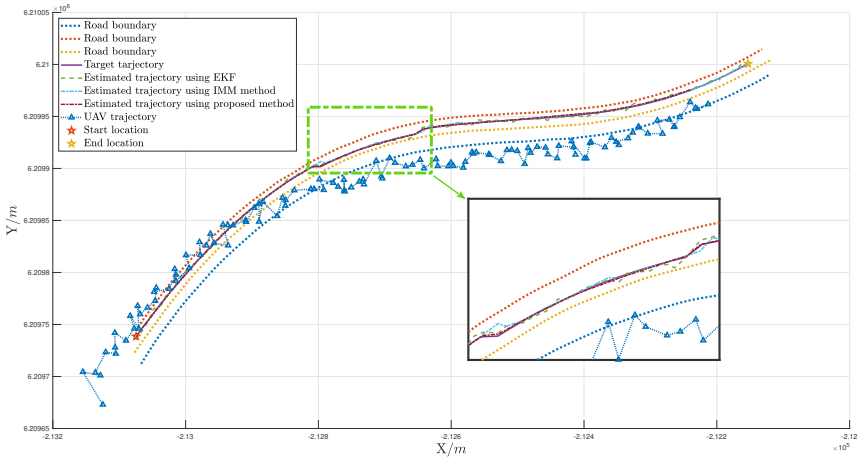


Fig. 11: Target tracking scenario

also shows that compared with IMM method, proposed method can automatically match the correct domain constrained information and demonstrates a strong robustness toward dynamic changes of terrain conditions.

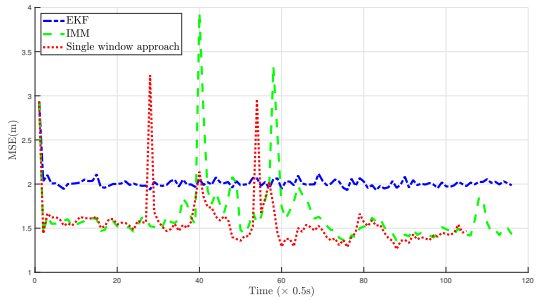
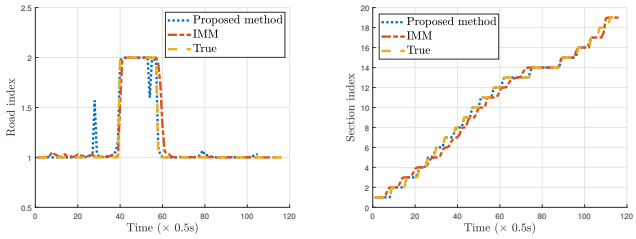


Fig. 12: MDE results of single window method



(a) Lane index inference of single window method

(b) Section index inference of single window method

Fig. 13: Constraint inference result (single window method)

However, it is important to note that proposed method exhibits significant performance degradation at certain time instances, namely 14s, 20s, 27s, 30s, and 40s, as shown in Fig. 12. Analysis of the ground target's driving behavior in the first scenario suggests that the performance degradation at 20s and 30s is probably due to the lane-changing behavior, which violates the original constraints and renders the domain constrained information ineffective. And this hypothesis is

TABLE II: Performance comparison

Method	MDE		RMSE	
	mean	std	mean	std
EKF	2.0153	0.0942	2.2861	0.0737
IMM	1.6412	0.3627	1.9495	0.3294
Single window	1.5621	0.2940	1.8870	0.3055
Double window	**1.5358**	0.2145	**1.8480**	0.1945

verified by the same performance degradation demonstrated by the constrained filter with IMM logic in Fig. 12. The performance degradation at 14s, 27s, and 40s can be observed in both Fig. 12 and Fig. 13a, indicating that the peaks in Fig. 12 are likely caused by the domain knowledge inference noise. Additionally, these time instances coincide with the edge of the sliding window. Thus, we may conclude that the performance degradation at 14s, 27s, and 40s are a result of the edge effect mentioned in Section III-C.

D. Performance evaluation of double window tracker

To further alleviate the edge effect and improve tracking accuracy, we investigate the performance of the double sliding window tracking approach. The results of MDE and terrain information inference after 1000 Monte Carlo simulations are shown in Fig. 14 and Fig. 15, respectively. It is observed that the performance degradation caused by the edge effect is effectively mitigated, resulting in an improved tracking performance. For comparison, the overall tracking performances of the EKF, single window approach, constrained IMM filter and double window approach are summarized in Table II. It shows that proposed methods yield the better tracking performance than other unconstrained and constrained filters, and the double window method successfully mitigates the edge effect and achieves better results than the single window approach.

E. Anomalous behavior recognition

The performance of anomaly driving pattern detection leveraging domain information is verified here. To comprehensively

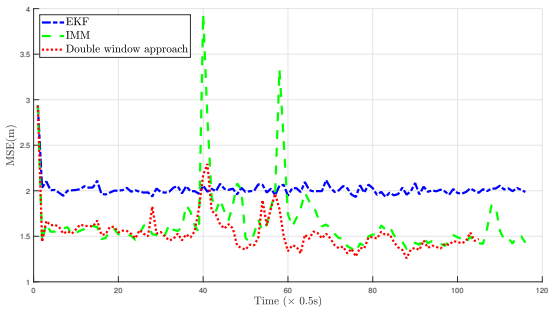
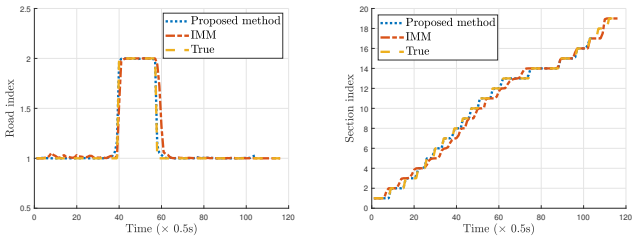


Fig. 14: MDE results of double window method



(a) Lane index inference of double window method

(b) Section index inference of double window method

Fig. 15: Constraint inference result (double window method)

explore performance of proposed method, both tracking scenarios proposed in Section V-A are utilized for comparison purposes. The target driving behavior database $\mathcal{D}$ consisting of N=10000 driving patterns is subsequently generated using a random walk logic with the Markov model defined in Fig. 16 and 18. To further emphasis the effectiveness of proposed method in this application, we leverage the string matching method proposed in [33] for comparison purpose. The simulation results are shown in Fig. 17. The anomalous level remains lowest when the target is performing the commonly used behavior, i.e., the straight forward driving action. In the first scenario, the target performs an overtaking behavior from 20s to 30s, resulting in a rise of anomalous value in 20s and 30s, which, in accordance with cognition, neither triggers alert nor monitor alarm. However, in the second tracking scenario, the ground target performs lane changing behavior twice, driving onto the adjacent lane at 20s, which is a normal behavior with no anomaly detected, while directly entering the opposite lane at 40s, clearly violating the traffic regulation. This law-breaking behavior does not trigger alert with string matching method (as the maneuver sequence appears to be normal), but is successfully detected by proposed method, illustrating the effectiveness of the anomaly detection mechanism in this tracking application.

VI. Conclusion

This paper presents a novel framework for tracking ground targets and anomalous driving behavior recognition using a UAV, with the aid of dynamic terrain information. The proposed method models the target state and external constraints on its motion imposed by domain knowledge using Hidden

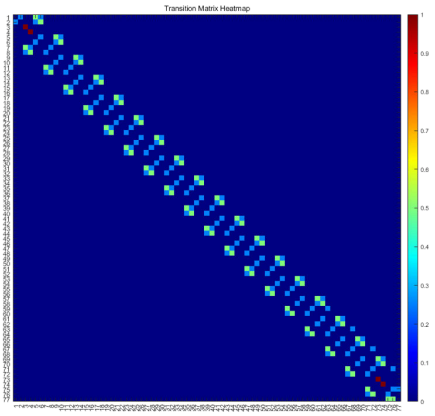


Fig. 16: Transition matrix

Markov Models (HMM), and infers the domain constraints by employing a lightweight Viterbi algorithm. After extracting the correct domain information, a constrained on-road filter is utilized to enforce both the target state and propagation process to comply with the domain constraints, leading to improved target tracking accuracy. Subsequently, using the terrain information inference results and domain knowledge, an efficient anomalous driving behavior recognition mechanism is seamlessly integrated, thereby increasing the UAV's autonomy. Simulation results demonstrate the proposed method's robustness towards changes in domain constrained knowledge, and promising results are achieved for both target tracking and anomaly detection.

One of the major limitations of our work is that only single UAV for single target tracking is considered. This method, though effective and easy for implementation, can be further improved in terms of tracking accuracy, flexibility and coverage with the cooperation of other intelligent units. In the future research, the scope will be extended by considering dynamic tracking scenario with multiple targets and UAVs. In this case, a comprehensive strategy trading-off between tracking efficiency and robustness while maintaining the consistency of UAV swarm will be tailored for complex tracking scenarios. Besides, only simulated data is used for verification in this paper, the future study will employ motion capture system for further indoor experimental data collection and tracking tests.

Acknowledgment

This work was supported by the National Natural Science Foundation of China under Grant No. 52302449. The authors would like to thank Yue Hou for his contributions to simulation setup and effective discussions in the aspect of machine learning.

References

[1] N. Miller and J. Rogers, "Simultaneous tracking of multiple ground targets from a multirotor unmanned aerial vehicle," *Journal of Aerospace Information Systems*, vol. 12, no. 3, pp. 345–364, 2015.

[2] V. Lappas, H.-S. Shin, A. Tsourdos, D. Lindgren, S. Bertrand, J. Marzat, H. Piet-Lahanier, Y. Daramouskas, and V. Kostopoulos, "Autonomous unmanned heterogeneous vehicles for persistent monitoring," *Drones*, vol. 6, no. 4, p. 94, 2022.

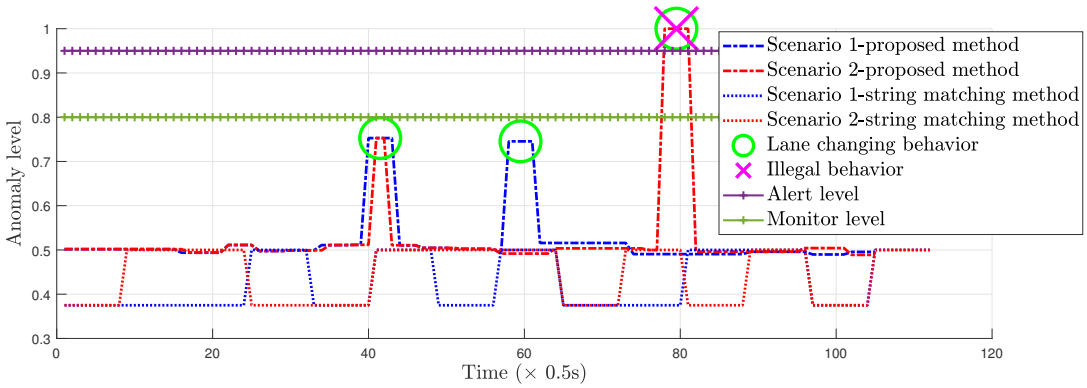


Fig. 17: Anomaly detection result

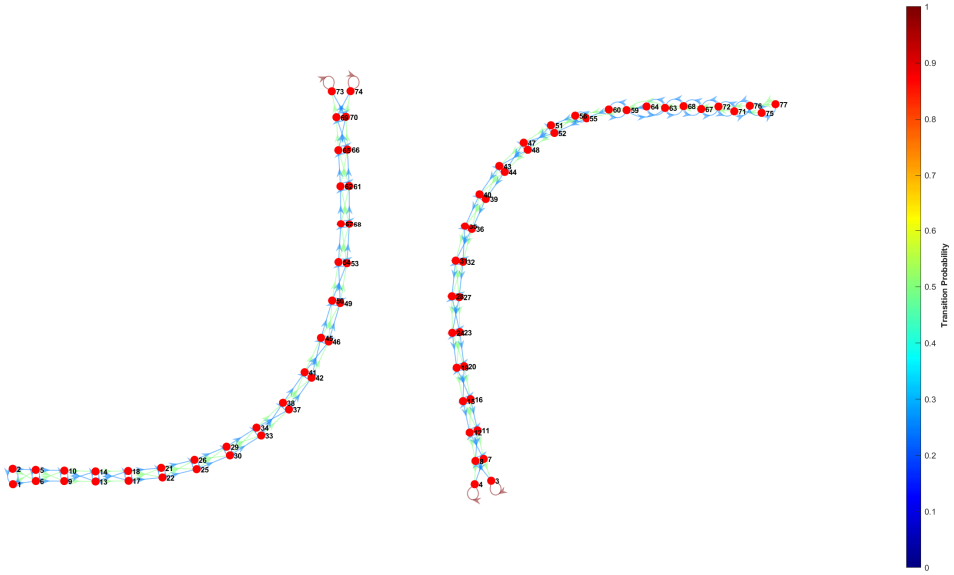


Fig. 18: Section switch preference simulation (The red nodes represent road sections corresponding to Fig. 10. The directional arrows are employed to signify transitions between section modes, wherein varying colors are employed to denote distinct transition probabilities. The color gradient, ranging from blue to red, is representative of the spectrum of values extending from 0 to 1.)

[3] N. Chen, F. Kong, W. Xu, Y. Cai, H. Li, D. He, Y. Qin, and F. Zhang, "A self-rotating, single-actuated uav with extended sensor field of view for autonomous navigation," *Science Robotics*, vol. 8, no. 76, p. eade4538, 2023. [Online]. Available: https://www.science.org/doi/abs/10.1126/scirobotics.ade4538

[4] H. Shakhatreh, A. H. Sawalmeh, A. Al-Fuqaha, Z. Dou, E. Almaita, I. Khalil, N. S. Othman, A. Khreishah, and M. Guizani, "Unmanned aerial vehicles (uavs): A survey on civil applications and key research challenges," *IEEE Access*, vol. 7, pp. 48 572–48 634, 2019.

[5] M. Popović, "Counting penguins with drones," *Science Robotics*, vol. 5, no. 47, p. eabe7458, 2020.

[6] H.-S. Shin, D. Turchi, S. He, and A. Tsourdos, "Behavior monitoring using learning techniques and regular-expressions-based pattern matching," *IEEE Transactions on Intelligent Transportation Systems*, vol. 20, no. 4, pp. 1289–1302, 2018.

[7] H.-S. Shin, A. J. Garcia, and S. Alvarez, "Information-driven persistent sensing of a non-cooperative mobile target using uavs," *Journal of Intelligent & Robotic Systems*, vol. 92, pp. 629–643, 2018.

[8] H. Oh and S. Kim, "Persistent standoff tracking guidance using constrained particle filter for multiple uavs," *Aerospace Science and Technology*, vol. 84, pp. 257–264, 2019.

[9] H. Oh, S. Kim, and A. Tsourdos, "Road-map–assisted standoff tracking of moving ground vehicle using nonlinear model predictive control," *IEEE Transactions on Aerospace and Electronic Systems*, vol. 51, no. 2, pp. 975–986, 2015.

[10] M. Ulmke and W. Koch, "Road-map assisted ground moving target tracking," *IEEE Transactions on Aerospace and Electronic Systems*, vol. 42, no. 4, pp. 1264–1274, 2006.

[11] A. Farina, "Application of knowledge-based techniques to tracking function," Selex Sistemi Integrati Rome (ITALY), Tech. Rep., 2006.

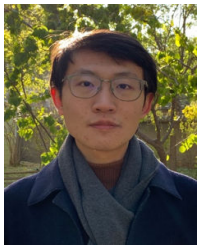
[12] C. Yang, M. Bakich, and E. Blasch, "Nonlinear constrained tracking of targets on roads," in *2005 7th International Conference on Information Fusion*, vol. 1. IEEE, 2005, pp. 8–pp.

[13] M. Mertens and M. Ulmke, "Precision gmti tracking using road constraints with visibility information and a refined sensor model," in *2008 IEEE Radar Conference*. IEEE, 2008, pp. 1–6.

[14] Y. Chen, V. P. Jilkov, and X. R. Li, "Multilane-road target tracking using radar and image sensors," *IEEE Transactions on Aerospace and Electronic Systems*, vol. 51, no. 1, pp. 65–80, 2015.

[15] G. Zhou, K. Li, T. Kirubarajan, and L. Xu, "State estimation with trajectory shape constraints using pseudomeasurements," *IEEE Transactions on Aerospace and Electronic Systems*, vol. 55, no. 5, pp. 2395–2407,

2018.
[16] M. Tahk and J. L. Speyer, "Target tracking problems subject to kinematic constraints," *IEEE Transactions on Automatic Control*, vol. 35, no. 3, pp. 324–326, 1990.
[17] D. Simon and T. L. Chia, "Kalman filtering with state equality constraints," *IEEE transactions on Aerospace and Electronic Systems*, vol. 38, no. 1, pp. 128–136, 2002.
[18] T. Kirubarajan, Y. Bar-Shalom, K. R. Pattipati, and I. Kadar, "Ground target tracking with variable structure imm estimator," *IEEE Transactions on Aerospace and Electronic Systems*, vol. 36, no. 1, pp. 26–46, 2000.
[19] M. S. Arulampalam, N. Gordon, M. Orton, and B. Ristic, "A variable structure multiple model particle filter for gmti tracking," in *Proceedings of the Fifth International Conference on Information Fusion. FUSION 2002.(IEEE Cat. No. 02EX5997)*, vol. 2. IEEE, 2002, pp. 927–934.
[20] X. Shao, B. Huang, and J. M. Lee, "Constrained bayesian state estimation–a comparative study and a new particle filter based approach," *Journal of Process Control*, vol. 20, no. 2, pp. 143–157, 2010.
[21] M. Yu, H. Oh, and W.-H. Chen, "An improved multiple model particle filtering approach for manoeuvring target tracking using airborne gmti with geographic information," *Aerospace Science and technology*, vol. 52, pp. 62–69, 2016.
[22] S. Ko and R. R. Bitmead, "State estimation for linear systems with state equality constraints," *Automatica*, vol. 43, no. 8, pp. 1363–1368, 2007.
[23] C. V. Rao, J. B. Rawlings, and J. H. Lee, "Constrained linear state estimation—a moving horizon approach," *Automatica*, vol. 37, no. 10, pp. 1619–1628, 2001.
[24] R. Zanetti, M. Majji, R. H. Bishop, and D. Mortari, "Norm-constrained kalman filtering," *Journal of Guidance, Control, and Dynamics*, vol. 32, no. 5, pp. 1458–1465, 2009.
[25] T. Li, "Single-road-constrained positioning based on deterministic trajectory geometry," *IEEE Communications Letters*, vol. 23, no. 1, pp. 80–83, 2018.
[26] J. Zhou, T. Li, X. Wang, and L. Zheng, "Target tracking with equality/inequality constraints based on trajectory function of time," *IEEE Signal Processing Letters*, vol. 28, pp. 1330–1334, 2021.
[27] A. Calise, "Enforcing an algebraic constraint in extended kalman filter design," in *AIAA Guidance, Navigation and Control Conference and Exhibit*, 2007, p. 6515.
[28] D. Simon, "Kalman filtering with state constraints: a survey of linear and nonlinear algorithms," *IET Control Theory & Applications*, vol. 4, no. 8, pp. 1303–1318, 2010.
[29] J. Chai, S. He, and H.-S. Shin, "Domain-knowledge-aided airborne ground moving targets tracking," *arXiv preprint arXiv:2303.06593*, 2023.
[30] B. Pannetier, K. Benameur, V. Nimier, and M. Rombaut, "Vs-imm using road map information for a ground target tracking," in *2005 7th International Conference on Information Fusion*, vol. 1. IEEE, 2005, pp. 8–pp.
[31] R. Chalapathy and S. Chawla, "Deep learning for anomaly detection: A survey," *arXiv preprint arXiv:1901.03407*, 2019.
[32] S. Ucar, B. Hoh, and K. Oguchi, "Abnormal driving behavior detection system," in *2021 IEEE 93rd Vehicular Technology Conference (VTC2021-Spring)*. IEEE, 2021, pp. 1–6.
[33] H. Oh, S. Kim, H.-S. Shin, A. Tsourdos, and B. A. White, "Behaviour recognition of ground vehicle using airborne monitoring of unmanned aerial vehicles," *International Journal of Systems Science*, vol. 45, no. 12, pp. 2499–2514, 2014.
[34] F. Katsilieris and A. Charlish, "Knowledge based anomaly detection for ground moving targets," in *2018 IEEE Radar Conference (RadarConf18)*. IEEE, 2018, pp. 0786–0791.
[35] F. Katsilieris, H. Driessen, and A. Yarovoy, "Threat-based sensor management for target tracking," *IEEE Transactions on Aerospace and Electronic Systems*, vol. 51, no. 4, pp. 2772–2785, 2015.
[36] H. Oh, H.-S. Shin, S. Kim, A. Tsourdos, and B. A. White, "Airborne behaviour monitoring using gaussian processes with map information," *IET Radar, Sonar & Navigation*, vol. 7, no. 4, pp. 393–400, 2013.
[37] C. Yang, A. Renzaglia, A. Paigwar, C. Laugier, and D. Wang, "Driving behavior assessment and anomaly detection for intelligent vehicles," in *2019 IEEE International Conference on Cybernetics and Intelligent Systems (CIS) and IEEE Conference on Robotics, Automation and Mechatronics (RAM)*. IEEE, 2019, pp. 524–529.
[38] S. M. Ross, *Introduction to probability models*. Academic press, 2014.
[39] S. He, H.-S. Shin, and A. Tsourdos, "Trajectory optimization for target localization with bearing-only measurement," *IEEE Transactions on Robotics*, vol. 35, no. 3, pp. 653–668, 2019.
[40] S. Ponda, R. Kolacinski, and E. Frazzoli, "Trajectory optimization for target localization using small unmanned aerial vehicles," in *AIAA Guidance, Navigation, and Control Conference*, 2009, p. 6015.
[41] D. M. Hawkins, *Identification of outliers*. Springer, 1980, vol. 11.
[42] A. Viterbi, "Error bounds for convolutional codes and an asymptotically optimum decoding algorithm," *IEEE Transactions on Information Theory*, vol. 13, no. 2, pp. 260–269, 1967.
[43] T. Chen, "Comments on "state estimation for linear systems with state equality constraints"[automatica 43 (2007) 1363–1368]," *Automatica*, vol. 46, no. 11, pp. 1929–1932, 2010.
[44] S. He, H.-S. Shin, S. Xu, and A. Tsourdos, "Distributed estimation over a low-cost sensor network: A review of state-of-the-art," *Information Fusion*, vol. 54, pp. 21–43, 2020.
[45] Y. Bar-Shalom, X. R. Li, and T. Kirubarajan, *Estimation with applications to tracking and navigation: theory algorithms and software*. John Wiley & Sons, 2001.
[46] S. He, H.-S. Shin, and A. Tsourdos, "Information-theoretic joint probabilistic data association filter," *IEEE Transactions on Automatic Control*, vol. 66, no. 3, pp. 1262–1269, 2020.
[47] S. S. Blackman and R. Popoli, *Design and analysis of modern tracking systems*. Norwood, MA: Artech House, 1999.
[48] S. He, H.-S. Shin, and A. Tsourdos, "Distributed joint probabilistic data association filter with hybrid fusion strategy," *IEEE Transactions on Instrumentation and Measurement*, vol. 69, no. 1, pp. 286–300, 2019.



Jianduo Chai received his B.Sc. degree in Detection, Guidance, and Control Technology from Beijing Institute of Technology in 2017. Currently, he is pursuing an M.Sc. degree at the School of Aerospace Engineering, Beijing Institute of Technology. His research focuses on multiple target tracking, navigation and trajectory optimization of autonomous systems.

Dr. He received the *Lord Kings Norton Medal* award from Cranfield University as the most outstanding doctoral student in 2020.



Shaoming He received the B.Sc. degree and the M.Sc. degree in aerospace engineering from Beijing Institute of Technology, Beijing, China, in 2013 and 2016, respectively, and the Ph.D. degree in aerospace engineering from Cranfield University, Cranfield, U.K., in 2019. He is currently an Associate Professor with School of Aerospace Engineering, Beijing Institute of Technology and also a recognized teaching staff with School of Aerospace, Transport and Manufacturing, Cranfield University. His research interests include aerospace guidance, multitarget tracking and trajectory optimization.

Dr. He received the *Lord Kings Norton Medal* award from Cranfield University as the most outstanding doctoral student in 2020.



Hyo-Sang Shin received the B.Sc. degree in aerospace engineering from Pusan National University, Busan, South Korea, in 2004, the M.Sc. degree in aerospace engineering with focus on flight dynamics, guidance, and control from Korea Advanced Institute of Science and Technology (KAIST), Daejeon, South Korea, in 2006, and the Ph.D. degree in cooperative missile guidance from Cranfield University, Cranfield, U.K., in 2010.

He is currently Head of Autonomous and Intelligent Systems Group and a Professor of Guidance, Navigation and Control with Cranfield University. His research interests include multiple target tracking, probabilistic target detection, and distributed control of multiple agent systems.

Dr. Shin is an Associate editor of *IEEE Transactions on Aerospace and Electronic Systems* and *Journal of Intelligent and Robotic Systems*.



Antonios Tsourdos obtained a MEng in electronic, control and systems engineering from the University of Sheffield (1995), an MSc in systems engineering from Cardiff University (1996), and a PhD in nonlinear robust missile autopilot design and analysis from Cranfield University (1999). He is a Professor of Control Engineering with Cranfield University, and was appointed Head of the Centre for Cyber-Physical Systems in 2013.

Dr. Tsourdos was a member of the Team Stellar, the winning team for the UK MoD Grand Challenge (2008) and the IET Innovation Award (Category Team, 2009). He is an Associate editor of *IEEE Transactions on Aerospace and Electronic Systems*, *Proceedings of the IMechE Part G: Journal of Aerospace Engineering*, *Aerospace Science & Technology*, and *International Journal of Systems Science*.



https://dspace.org/

Dynamic knowledge-based tracking and autonomous anomaly detection

Chai, Jianduo; He, Shaoming; Shin, Hyo-Sang; Tsourdos, Antonios

2023-11-28
Institute of Electrical and Electronics Engineers (IEEE)
https://doi.org/10.1109/TAES.2023.3337190
Chai J, He S, Shin HS, Tsourdos A. (2024) Dynamic knowledge-based tracking and autonomous anomaly detection. IEEE Transactions on Aerospace and Electronic Systems, Volume 60, Issue 2, April 2024, pp. 1597-1611

Downloaded from a DSpace repository. https://dspace.org/